

Synthesis and characterization of a novel type of self-assembled chiral zirconium phosphonates and its application for heterogeneous asymmetric catalysis

Xinjun Wu, Xuebing Ma*, Yeling Ji, Qiang Wang, Xiao Jia, Xiangkai Fu

College of Chemistry and Chemical Engineering, Southwest University, Chongqing 400715, PR China

Received 8 May 2006; received in revised form 14 July 2006; accepted 11 October 2006

Available online 19 October 2006

Abstract

A readily available (1*S*,2*R*)-(+)-2-amino-1,2-diphenylethanol and (1*R*,2*S*)-(–)-2-amino-1,2-diphenylethanol were immobilized on the layered zirconium phosphonates and the hybrid chiral zirconium phosphonates framework had been synthesized for the first time. The solid catalysts were characterized by IR, AFM, TG, XRD and elemental analysis. AFM showed that the self-assembled structure of chiral organic ligands on the surface of zirconium phosphonates **4** lined up regularly and homogeneously at 1.1 nm distance. XRD data indicated that zirconium phosphonate **4** was semi-crystalline with the interlayer space 20.11 Å. Zirconium phosphonates **4** enantioselectively catalyzed the addition of Et₂Zn to benzaldehyde to afford optical secondary alcohol in >90% yield and 51% e.e. which only decrease at 6% enantiomeric excess lower than the corresponding chiral ligand (1*R*,2*S*)-(–)-**2** in homogeneous asymmetric catalysis.

© 2006 Elsevier B.V. All rights reserved.

Keywords: Self-assembled; Chiral; Immobilized; Zirconium phosphonate; Enantioselective addition

1. Introduction

Heterogeneous chiral catalysts which are friendly to the environment have the inherent advantages of the easier handling, separation and recovery from the reaction mixture over the homogeneous catalysts. Current research on preparation of heterogeneous chiral catalysts is very active and needed in pharmaceutical, food, and agricultural industries [1,2]. The immobilization of the chiral auxiliaries on different polymer supports [3–6] and silica [7–11] have recently attracted great attention for synthetic chemists because of their engineering interesting properties. However, the former is limited above the temperature of 120 °C and the latter is easy to lose activity due to their breaking off.

Zirconium phosphate is known to exist in two common forms: α -zirconium phosphate (α -ZrP, Zr(HPO₄)₂·H₂O) and γ -zirconium phosphate (γ -ZrP, Zr(PO₄)(H₂PO₄)₂·2H₂O) [12–14]. A variety of zirconium phosphonates Zr(HPO₄)_{2–x}(O₃PR)_x·nH₂O (R is organic group) with the surface areas of 30–200 m²/g pos-

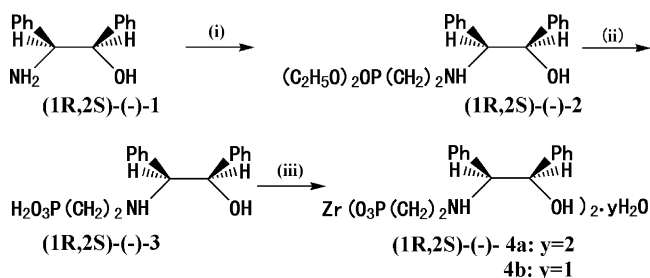
sessing the α -structure where the interlamellar OH group is simply replaced by an organic moiety [15] have been prepared. All organic groups in the zirconium phosphonates are located on the surface of the layer and the interlamellar region which are very useful for catalysis. The application of zirconium phosphonates was focused on the solid acid catalysis [16–20], solid base catalysis [21] and hydrogenation reactions [22,23]. Seldom was reported on the application of the zirconium phosphonates in the field of asymmetric catalysis [24,25]. In this paper, the (1*S*,2*R*)-(+)-2-amino-1,2-diphenylethanol and (1*R*,2*S*)-(–)-2-amino-1,2-diphenylethanol were immobilized by covalent bonding on inorganic layered support to afford zirconium phosphonates **4** and hybrid zirconium phosphonates **5** [Zr(O₃P \emptyset)_{2–x}(O₃PR)_x·yH₂O, \emptyset is *N*-ethyl-2-imino-1,2-diphenylethanol and R is ethyl group] (Schemes 1 and 2), and the enantioselective addition of diethylzinc to benzaldehyde had also been detailed.

2. Experimental

2.1. Starting materials and methods

(1*S*,2*R*)-(+)-2-amino-1,2-diphenylethanol ($[\alpha]_D^{20} = +8.0^\circ$, c 2.13, CHCl₃), (1*R*,2*S*)-(–)-2-amino-1,2-diphenylethanol

* Corresponding author. Tel.: +86 23 68253237; fax: +86 23 68254000.
E-mail addresses: wj2004@swu.edu.cn, zcyj123@swu.edu.cn (X. Ma).

Scheme 1. The preparation of chiral zirconium phosphonates **4**.

$[\alpha]_D^{20} = -8.36^\circ$, c 2.13, CHCl_3) was supplied by Astara Company. Diethyl ethylphosphonate (99%, Fluka) was used without further purification. Diethyl-2-bromoethyl phosphonate $[\text{BrCH}_2\text{CH}_2\text{P}(\text{O})(\text{OEt})_2]$ was synthesized by reaction of triethylphosphite with 1,2-dibromoethane according to literature [26]. All other materials used are of analytical grade.

Infrared spectra were recorded on Spectrum GX using polystyrene as a standard (KBr pellet). TG analyses were performed on a SBTQ600 Thermal Analyzer (USA) with the heating rate of $20^\circ\text{C min}^{-1}$ to 1000°C under flowing N_2 (100 ml min^{-1}). ^1H , ^{13}C and ^{31}P NMR were performed on a Broker AV-300 NMR instrument at ambient temperature at 300, 75 and 121 MHz, respectively. All of the chemical shifts were reported downfield in ppm relative to the hydrogen, carbon and phosphorus resonance of TMS, chloroform- d_1 and 85% H_3PO_4 , respectively. The interlayer spacings were obtained on a Phillips (model 1710) semiautomatic X-ray power diffractometer using $\text{Cu K}\alpha$ radiation with a scanning speed of 2° min^{-1} . Atomic force microscopy was carried out on a Multimode SPM Veew instruments Inc. (USA). C, H and N elemental analysis were obtained from an EATM 1112 Automatic Elemental Analyzer (Thermo, USA) instrument. GC analysis was performed on an Agilent6820 gas chromatograph (USA) using a 30 m Chiral Cyclodex-B capillary column: temperature program 70°C , 5 min, 3°C min^{-1} , 160°C , 35 min. Optical rotations were determined on a Perkin-Elmer 341 polarimeter.

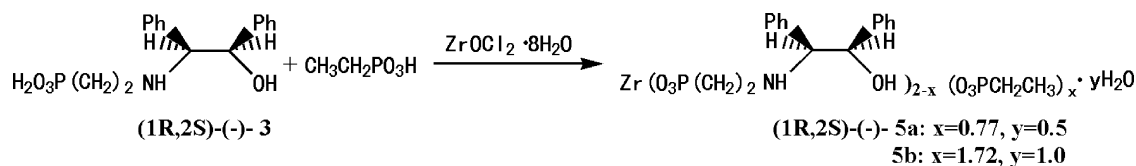
The molar ratio of organic moiety diphenylethanol/ethyl in the zirconium phosphonate **5** was obtained by ^{31}P NMR measurements after dissolution of a weighed amount of sample (30 mg) in a few drops of concentrated HF and about 0.5 ml of D_2O as solvent. The shifts of the signals of (1*S*,2*R*)-(+)-*N*-ethylphosphonic acid-2-imino-1,2-diphenylethanol and ethylphosphonic acid were 24.1 and 35.3 ppm, respectively. A suitable time delay ($d_1 = 5$) was set to ensure quantitative measurements. The shifts are relative to 85% H_3PO_4 in D_2O .

2.2. Synthesis of (1*S*,2*R*)-(+)-*N*-(diethyl ethylphosphonate)-2-imino-1,2-diphenylethanol and (1*R*,2*S*)-(-)-*N*-(diethyl ethylphosphonate)-2-imino-1,2-diphenylethanol (**2**)

To 100 ml ethanol solution of (1*S*,2*R*)-(+)-2-amino-1,2-diphenylethanol or (1*R*,2*S*)-(-)-2-amino-1,2-diphenylethanol (4.26 g, 20 mmol) was added a catalytic amount of sodium iodide and diethyl-2-bromoethyl phosphonate (9.00 g, 40 mmol). The reaction mixture was stirred for 6–7 days at $50\text{--}60^\circ\text{C}$ with the tracking of TLC and the solution of sodium carbonate (1 mol L^{-1}) was used to maintain pH in the range of 7–8. Then the reaction mixture was extracted by CHCl_3 ($30\text{ ml} \times 3$), the organic phase was combined and concentrated under reduced pressure. The crude product was purified by recrystallizing with ethyl acetate, filtered, dried in vacuo to obtain white crystals of 6.67 g (1*S*,2*R*)-(+)-**2** and 6.91 g (1*R*,2*S*)-(-)-**2** in 88.5% and 91.6% yield, respectively. m.p. $126\text{--}127^\circ\text{C}$, $[\alpha]_D^{25} = +35.6^\circ$ [(1*S*,2*R*)-(+)-**2**, c 3.77, CHCl_3], $[\alpha]_D^{25} = -23.6^\circ$ [(1*R*,2*S*)-(-)-**2**, c 3.77, CHCl_3]. ^1H NMR (CDCl_3): δ 7.29–7.24 (6H, m), 7.15–7.09 (4H, m), 4.90 (OCH, 1H, d, $^3J = 6.0\text{ Hz}$), 4.04 (OCH₂, 4H, m), 3.99 (NCH, 1H, d, $^3J = 5.4\text{ Hz}$), 2.80 (NCH₂, 2H, m), 2.01 (NH, 1H, m), 1.93 (CH₂P, 2H, m), 1.27 (CH₃, 6H, t, $^3J = 5.4\text{ Hz}$). ^{31}P NMR (CDCl_3): 31.7. ^{13}C NMR (CDCl_3): 140.3, 138.7, 128.3, 127.8, 127.6, 126.9 (–Ph), 76.5 (OCH), 68.4 (OCH₂), 61.7 (NCH), 40.9 (d, $^2J_{\text{C-P}} = 18\text{ Hz}$, NCH₂), 26.4 (d, CH₂P, $^1J_{\text{C-P}} = 558\text{ Hz}$), 16.5 (d, CH₃, $^3J_{\text{C-P}} = 21\text{ Hz}$). IR (KBr, ν , cm^{-1}): 3335 (m), 3064 (s), 3026 (s), 2983 (s), 2925 (m), 2872 (m), 1599 (m), 1548 (m), 1494 (m), 1452 (m), 1390 (s), 1291 (s), 1026 (s), 704 (s), 676 (w).

2.3. Preparation of chiral zirconium phosphonate **4a**

A mixture of (1*S*,2*R*)-(+)-**2** or (1*R*,2*S*)-(-)-**2** (3.77 g, 10 mmol), acetic acid (150 ml) and hydrochloric acid (36%, 30 ml) was stirred for 8 h at 80°C . Then the solution of zirconium oxychloride (1.62 g, 5 mmol) in deionized water (80 ml) was added dropwise with stirring. The reaction mixture was kept at $70\text{--}80^\circ\text{C}$ for 24 h, filtered, washed with sodium bicarbonate solution, water to pH in the range of 6–7 and thrice with ethanol ($30\text{ ml} \times 3$). The white solid was dried in vacuo to obtain 3.53 g (1*S*,2*R*)-(+)-**4a** and 3.43 g (1*R*,2*S*)-(-)-**4b** in 92.3% and 89.6% yield, respectively. IR (KBr, ν , cm^{-1}): 3338 (s), 3063 (s), 3025 (s), 2928 (s), 2852 (s), 1603 (m), 1494 (m), 1455 (s), 1293 (m), 1029 (s), 704 (s), 667 (w). The anal. calcd. for (1*S*,2*R*)-(+)-**4a** ($\text{C}_{32}\text{H}_{40}\text{N}_2\text{O}_{10}\text{P}_2\text{Zr}$): C, 50.1; H, 5.26; N, 3.66. Found: C, 49.2; H, 5.10; N, 3.70. The anal. calcd. for (1*R*,2*S*)-(-)-**4a** ($\text{C}_{32}\text{H}_{40}\text{N}_2\text{O}_{10}\text{P}_2\text{Zr}$): C, 50.1; H, 5.26; N, 3.66. Found: C, 49.3; H, 5.12; N, 3.72.

Scheme 2. The preparation of the hybrid chiral zirconium phosphonates **5**.

2.4. Hydrothermal synthesis of chiral zirconium phosphonate **4b**

A mixture of (1*S*,2*R*)-(+)-**2** or (1*R*,2*S*)-(–)-**2** (0.377 g, 1 mmol), acetic acid (25 ml), zirconium oxychloride (0.322 g, 1 mmol) in deionized water (25 ml) and hydrochloric acid (36%, 10 ml) was added to a 100 ml stainless steel Teflon lined vessel. The reaction mixture was then sealed and heated at 120 °C for 48 h. The solid product was filtered, washed with sodium bicarbonate solution and water to pH in the range of 6–7 and thrice with ethanol (30 ml × 3). The white solid was dried in vacuo to obtain 0.346 g (1*S*,2*R*)-(+)-**4b** and 0.320 g (1*R*,2*S*)-(–)-**4b** in 85.6% and 87.8% yield, respectively. IR (KBr, ν , cm^{-1}): 3345 (s), 3063 (s), 3024 (s), 2929 (s), 2851 (s), 1603 (m), 1495 (m), 1454 (s), 1294 (m), 1030 (s), 704 (s), 675 (w). The anal. calcd. for (1*S*,2*R*)-(+)-**4b** ($\text{C}_{32}\text{H}_{38}\text{N}_2\text{O}_9\text{P}_2\text{Zr}$): C, 51.4; H, 5.12; N, 3.75. Found: C, 49.6; H, 5.08; N, 3.73. The anal. calcd. for (1*R*,2*S*)-(–)-**4b** ($\text{C}_{32}\text{H}_{38}\text{N}_2\text{O}_9\text{P}_2\text{Zr}$): C, 51.4; H, 5.12; N, 3.75. Found: C, 49.8; H, 5.02; N, 3.69.

2.5. Synthesis of hybrid chiral zirconium phosphonate **5**

A mixture of (1*S*,2*R*)-(+)-**2** or (1*R*,2*S*)-(–)-**2** (1.84 g, 5 mmol), diethyl ethylphosphonate (0.84 g, 5 mmol), acetic acid (150 ml) and hydrochloric acid (36%, 30 ml) was stirred for 8 h at 80 °C. Then the solution of zirconium oxychloride (1.62 g, 5 mmol) in 80 ml of deionized water was added dropwise with stirring. The reaction mixture was kept at 70–80 °C for 24 h, filtered, washed with sodium bicarbonate solution and water to pH in the range of 6–7 and thrice with ethanol (30 ml × 3). The white solid was dried in vacuo to obtain 2.07 g (1*S*,2*R*)-(+)-**5a** and 2.11 g (1*R*,2*S*)-(–)-**5a** in 88.5% and 90.2% yield, respectively, calculated according to compound **2**. IR (KBr, ν , cm^{-1}): (1*S*,2*R*)-(+)-**5a** 3424 (m), 3068 (s), 3028 (s), 2979 (s), 2930 (m), 2878 (m), 2850 (m), 1602 (m), 1582 (m), 1496 (m), 1453 (m), 1423 (s), 1293 (s), 1029 (s), 707 (s), 666 (w). The anal. calcd. for (1*S*,2*R*)-(+)-**5a** ($\text{C}_{21.22}\text{H}_{26.99}\text{N}_{1.23}\text{O}_{7.73}\text{P}_{2.0}\text{Zr}$): C, 44.2; H, 4.72; N, 2.99. Found: C, 39.9; H, 4.60; N, 2.70.

The molar ratio of (1*S*,2*R*)-(+)-**2** or (1*R*,2*S*)-(–)-**2** (1.84 g, 5 mmol) to diethyl ethylphosphonate (4.04 g, 24 mmol) was altered and carried out by the same synthetic step as above to obtain 4.36 g of (1*S*,2*R*)-(+)-**5b** and 4.45 g of (1*R*,2*S*)-(–)-**5b** in 82.2% and 84.0% yield, respectively, calculated according to diethyl ethylphosphonate. IR (KBr, ν , cm^{-1}): (1*S*,2*R*)-(+)-**5b** 3425 (m), 3058 (s), 3021 (s), 2978 (s), 2940 (s), 2884 (s), 2852 (m), 1605 (m), 1583 (m), 1495 (m), 1455 (m), 1416 (s), 1285 (s), 1036 (s), 707 (s), 668 (w). The anal. calcd. for (1*S*,2*R*)-(+)-**5b** ($\text{C}_{7.92}\text{H}_{15.64}\text{N}_{0.28}\text{O}_{7.28}\text{P}_{2.0}\text{Zr}$): C, 25.0; H, 4.15; N, 1.03. Found: C, 28.8; H, 4.30; N, 1.50.

2.6. General procedure for the enantioselective addition of Et_2Zn to benzaldehyde by using zirconium phosphonate **4a**

A 19.1 mg of (1*S*,2*R*)-(+)-**4a** (0.050 mmol) in anhydrous toluene (5 ml) was activated with stirring for 15 h at room temperature. Then the solution of Et_2Zn (0.50 ml, 2 mol l^{-1} in hexane solution) was added dropwise under an

argon atmosphere. After stirring for 3 h, benzaldehyde (1 ml, 0.5 mmol ml^{-1} in toluene) was added dropwise and the reaction was stirred for 72 h at room temperature. The reaction mixture was quenched by an addition of a saturated aqueous solution of NH_4Cl , filtered, extracted with ethyl acetate (5 ml × 3). The combined organic layer was washed with brine (10 ml), dried by anhydrous sodium sulfate and evaporated under reduced pressure to give an oily residue. The residue was purified by silica gel column using ethyl acetate/petroleum ether (60–90 °C) (5:1 (v/v)) to give optically active 1-phenyl-propanol.

2.7. Reusability of catalyst

A 286 mg of used catalyst (1*S*,2*R*)-(+)-**4a** was washed with hydrochloric acid (36%, 5 ml) to remove zinc oxide formed in the catalytic reaction and then with sodium bicarbonate solution and water to pH in the range of 6–7, dried in vacuo at 60–70 °C for 24 h to get 182 mg (1*S*,2*R*)-(+)-**4a** which can be reused for the enantioselective addition of Et_2Zn to benzaldehyde.

3. Results and discussion

3.1. Infrared spectra

Comparing the infrared spectra of the (1*S*,2*R*)-(+)-2-amino-1,2-diphenylethanol, (1*S*,2*R*)-(+)-**2**, the chiral zirconium phosphonates **4a** and **4b** and hybrid chiral zirconium phosphonates **5a** and **5b** (Fig. 1), it was found that all of them had the broad bands centered at $3425\text{--}3058\text{ cm}^{-1}$ which was

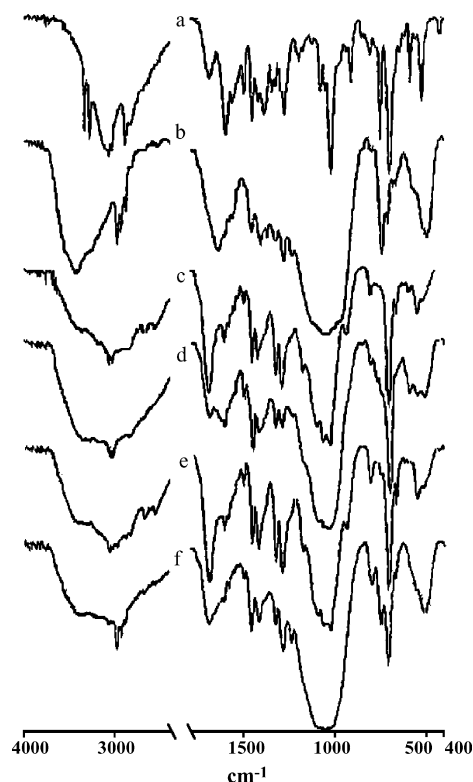


Fig. 1. The infrared spectra of the catalysts: (a) (1*S*,2*R*)-(+)-**1**; (b) (1*S*,2*R*)-(+)-**2**; (c) (1*S*,2*R*)-(+)-**4a**; (d) (1*S*,2*R*)-(+)-**4b**; (e) (1*S*,2*R*)-(+)-**5a**; (f) (1*S*,2*R*)-(+)-**5b**.

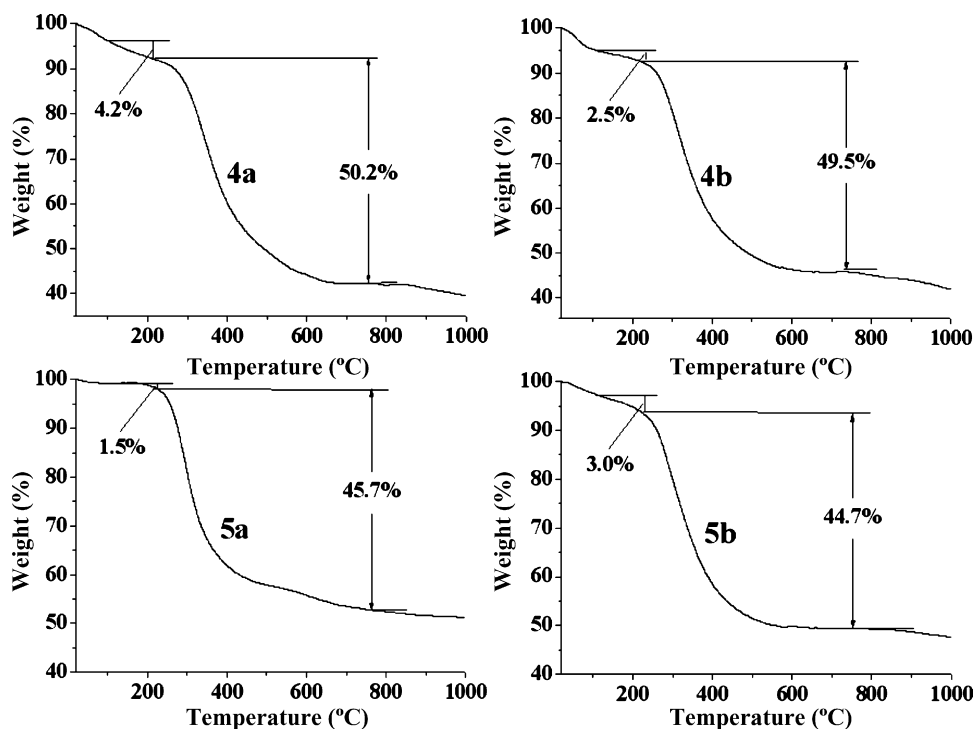


Fig. 2. Thermogravimetric analysis curve for zirconium phosphonate **4a** and **4b** and **5a** and **5b**.

attributed to the O–H and N–H stretching vibrations. The C–H stretching vibrations of the alkyl chain were clearly visible at about 2930 cm^{-1} . The broad band which extended from 2343 to 3714 cm^{-1} demonstrated that the hydrogen bond formed between hydroxy and amino group in 2-amino-1,2-diphenylethanol moiety each other on the surface [27]. IR spectra of these solids **4a**, **4b**, **5a** and **5b** exhibited strong and similar peaks at 960 – 1150 cm^{-1} owing to the P–O stretches vibration. It can be concluded that the similar structure of the solids **4a**, **4b**, **5a** and **5b** is kept and the organic group is present within the zirconium phosphonate framework.

3.2. Thermogravimetric analysis

On heating the samples (1*S*,2*R*)-(+)-**4a**, (1*S*,2*R*)-(+)-**4b**, (1*S*,2*R*)-(+)-**5a**, (1*S*,2*R*)-(+)-**5b**, the similar behaviors of their thermo-stability over a broad temperature range of 40 – $1000\text{ }^{\circ}\text{C}$ were observed. From the TG results showed in Fig. 2, it can be seen that the number of crystallization water in **4a**, **4b**, **5a** and **5b** were 2, 1, 0.5 and 1 H_2O unit individually according to the 4.2%, 2.5%, 1.5%, 3.0% weight loss of dehydration between 100 and $220\text{ }^{\circ}\text{C}$. The second peak with weight loss 50.2%, 49.5%, 45.7% and 44.7%, respectively, owing to the fragmentation of the appended organic groups took place in the temperature range of 220 – $750\text{ }^{\circ}\text{C}$. In the temperature range of 750 – $1000\text{ }^{\circ}\text{C}$ the losses were attributed to the dehydrolysis of $\text{Zr}(\text{HPO}_4)_2$ to ZrP_2O_7 .

For the hybrid derivatives **5a** and **5b**, the two types of pendant organic moieties do not pyrolyze discretely but instead volatilize together over a somewhat broadened range. So it is difficult to detect the content of the different pendant organic moieties by

the change in percent weight loss for hybrid zirconium phosphonates **5a** and **5b**. The amount of pendant organic moieties in hybrid **5a** and **5b** with $x=0.77$ and 1.72 was conformed by the values determined on the basis of ^{31}P NMR.

3.3. XRD results

The power XRD results (shown in Fig. 3, summarized in the Table 1) showed that both the chiral zirconium phosphonates **4** and hybrid chiral zirconium phosphonates **5** were regularly layered compounds and semi-crystalline with single strong diffraction peaks. The pure compounds **4a** and **4b** exhibited a simple XRD pattern in which the scattering angle was a direct

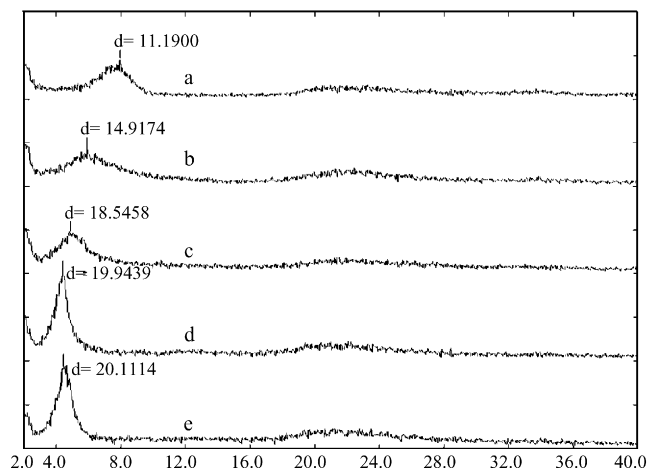


Fig. 3. X-ray diffraction pattern of zirconium phosphonate. (a) Zirconium ethylphosphonate; (b) **5b**; (c) **5a**; (d) **4b**; (e) **4a**.

Table 1
The interlayer space of chiral zirconium phosphonate **4** and hybrid chiral zirconium phosphonate **5**

Catalyst	Reactants			Method	<i>d</i> -Space (Å)	Formula ^a
	Zr (mmol)	\emptyset PO ₃ H (mmol) ^a	EtPO ₃ H (mmol)			
4a	10	10	0	Stirring	20.11	Zr(\emptyset PO ₃) ₂ ·2H ₂ O
4b	1	1	0	Hydrothermal	19.94	Zr(\emptyset PO ₃) ₂ ·H ₂ O
5a	10	10	10	Stirring	18.55	Zr(\emptyset PO ₃) _{1.23} (C ₂ H ₅ PO ₃) _{0.77} ·H ₂ O
5b	10	10	48	Stirring	14.92	Zr(\emptyset PO ₃) _{0.28} (C ₂ H ₅ PO ₃) _{1.72} ·H ₂ O
6^b	10	0	20	Stirring	11.19	Zr(C ₂ H ₅ PO ₃) ₂ ·H ₂ O

$\emptyset = (1S,2R)-(+)-2$.

^a By ³¹P NMR analysis.

^b Synthesized using the same method as **4a**.

measure of the *d* spacing with 20.11 and 19.94 Å, respectively, via the Bragg equation.

For a hybrid compound there are two different structural possibilities for distribution of the organic groups: (i) a random dispersion within the interlayer and all layers identical; (ii) an ordered segregation or staging of the organic groups into layers of distinct compositions. Each of these arrangements will give rise to characteristic features in the X-ray diffraction pattern. The randomly distributed structure will show a single 001 XRD peak whose *d* spacing is between the values observed for the two parent zirconium phosphonates [28]. Owing to the dilution of ethylphosphonate with shorter arm than chiral ligand (1*R*,2*S*)-(–)-**2** on the interlayer surface of zirconium plane, the interlayer spaces of zirconium phosphonates **4** and **5** [Zr(O₃P \emptyset)_{2–x}(O₃PR)_x·yH₂O, \emptyset is *N*-ethyl-2-imino-1,2-diphenylethanol and R is ethyl group] with single value decrease from 20.11 to 11.19 Å with the *x* increase from *x* = 0 to 0.77, 1.72 and 2.0, which demonstrated the distribution of the two type of organic moieties is a random dispersion.

3.4. Analysis of surface morphology

Scanning electron microscope (SEM) and atomic force microscopy (AFM) were used as the tools to understand the

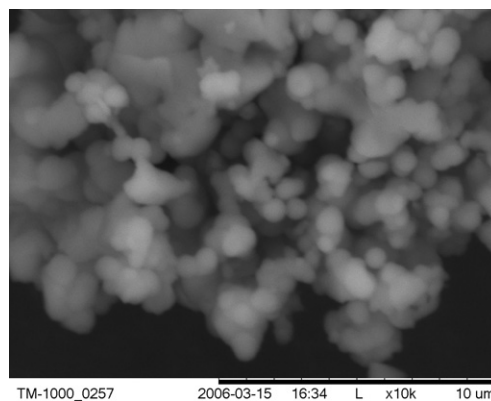
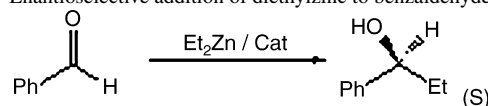


Fig. 4. SEM micrograph image of chiral zirconium phosphonate (1*S*,2*R*)-(+)-**4a**.

diameter of the catalyst (Fig. 4) and the distribution of the appended organic moieties on the surface (Fig. 5). SEM results showed that these materials were spheroid form and submicron in size. AFM showed that due to formation of hydrogen bond between 1,2-diphenyl-2-aminoethanol moieties each other on the surface of zirconium plane, the distribution of appended chiral organic moieties possessed interesting self-assembled structural features which lined regularly and homogeneously at 1.1 nm

Table 2
Enantioselective addition of diethylzinc to benzaldehyde using chiral zirconium phosphonate **4a**^a



Entry	Catalyst	Temperature (°C)	Time (h)	Yield (%) ^b	e.e. (%) ^c	Configuration ^d
1	(1 <i>S</i> ,2 <i>R</i>)-(+)- 4a	rt	72	91	51	<i>S</i>
2	(1 <i>S</i> ,2 <i>R</i>)-(+)- 4a	10	72	88	44	<i>S</i>
3	(1 <i>S</i> ,2 <i>R</i>)-(+)- 4a	0	72	80	36	<i>S</i>
4	(1 <i>S</i> ,2 <i>R</i>)-(+)- 4a	–10	72	66	25	<i>S</i>
5	(1 <i>R</i> ,2 <i>S</i>)-(–)- 4a	rt	12	65	37	<i>R</i>
6	(1 <i>R</i> ,2 <i>S</i>)-(–)- 4a	rt	24	68	35	<i>R</i>
7	(1 <i>R</i> ,2 <i>S</i>)-(–)- 4a	rt	48	83	42	<i>R</i>
8	(1 <i>R</i> ,2 <i>S</i>)-(–)- 4a	rt	96	92	33	<i>R</i>

^a Reaction was carried out in toluene with a molar ratio Et₂Zn/benzaldehyde/chiral ligand of catalyst = 2/1/0.1.

^b GC yield, determined by conversion times selectivity.

^c Determined by GC (30 m, Chiral Cyclodex-B column, Agilent).

^d Determined from the specific rotation of (*S*)-1-phenylpropanol: $[\alpha]_{\text{D}}^{25} = -47.6$ (6.11, CHCl₃) [29].

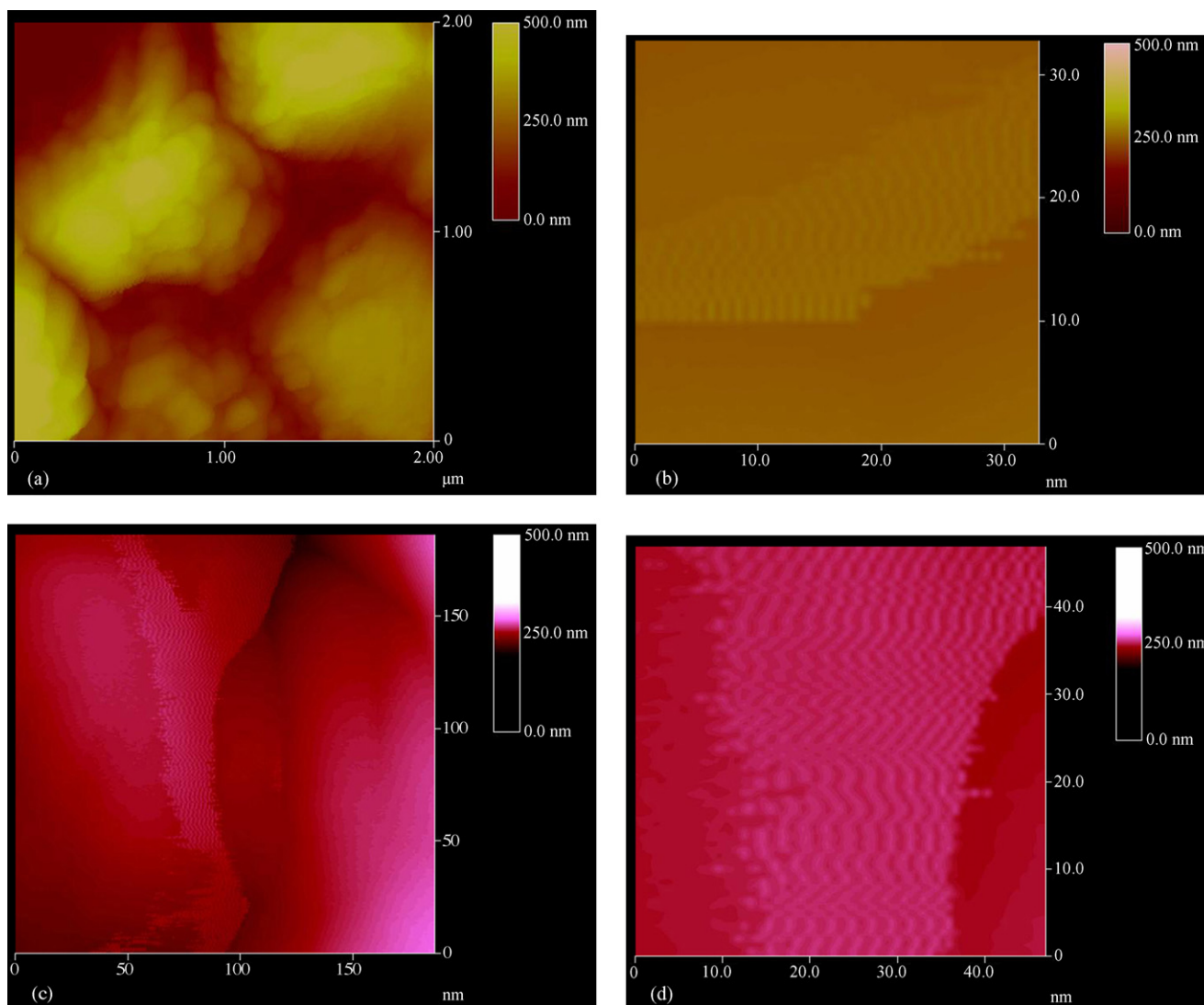


Fig. 5. AFM images of chiral zirconium phosphonate (1*S*,2*R*)-(+)-**4a**.

distance. And there were many ravines on the surface of (1*S*,2*R*)-(+)-**4a** which was very useful for catalysis.

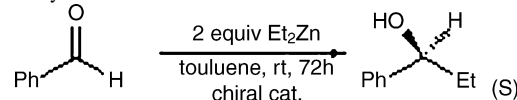
3.5. Enantioselective addition of diethylzinc to benzaldehyde

3.5.1. Activities and selectivities

The enantioselective addition reactions were carried out under the catalysis of the chiral zirconium phosphonate **4** (Table 2). From the catalytic reaction data, it was found that the isolated yield and enantiomer excess (e.e.%) increased with the reaction time and temperature. The reaction performed at room temperature for 72 h got the best yield (91%) and enantiomeric excess (51%) which was near to the corresponding homogeneous catalysis of (1*S*,2*R*)-(+)-**1** in 95% yield and 57% enantiomeric excess (Table 3, entry 7). The enantioselectivity in heterogenous catalytic system only decrease at 6% enantiomeric excess lower than those in homogeneous asymmetric catalysis. Taking into account that the catalytic site is formed via a zinc alcoholate obtained by reaction of the hydroxyl group of

Table 3

Enantioselective addition of diethylzinc to benzaldehyde catalyzed by different catalysts^a



Entry	Catalyst	Yield (%) ^b	e.e. (%) ^b	Configuration ^c
1	(1 <i>S</i> ,2 <i>R</i>)-(+)- 4a	91	51	<i>S</i>
2	(1 <i>R</i> ,2 <i>S</i>)-(–)- 4b	82	35	<i>R</i>
3	(1 <i>S</i> ,2 <i>R</i>)-(+)- 5a	74	28	<i>S</i>
4	(1 <i>R</i> ,2 <i>S</i>)-(–)- 5b	58	22	<i>R</i>
5	MIXZrP ^d	80	0	–
6	(1 <i>S</i> ,2 <i>R</i>)-(+)- 1	92	40	<i>S</i>
7	(1 <i>S</i> ,2 <i>R</i>)-(+)- 2	95	57	<i>S</i>

^a Reaction was carried out in toluene with a molar ratio Et₂Zn/benzaldehyde/chiral ligand of catalyst = 2/1/0.1.

^b Determined by GC (30 m, Chiral Cyclodex-B column, Agilent).

^c Absolute configuration assigned by comparison to the literatures.

^d Synthesized by the same way of preparing chiral hybrid zirconium phosphonate **5** with the reactants of (1*S*,2*R*)-(+)-**2** and phosphite in the molar ratio of 1:1.

Table 4
The catalytic activity of the reused chiral zirconium phosphonate (1*S*,2*R*)-(+)-**4a**

Time ^a	N _{PhCHO} (mmol)	Yield (%) ^b	e.e. (%) ^b	Configuration ^c
First	10.0	91	51	S
Second	9.5	88	50	S
Third	9.0	85	48	S
Fourth	8.5	79	45	S
Fifth	8.0	80	47	S
Sixth	7.5	78	46	S
Seventh	7.0	77	36	S
Eighth	6.5	75	32	S
Ninth	6.0	69	15	S
Tenth	5.0	49	12	S
Eleventh	4.0	28	0	S

^a The first reaction was carried out in toluene with a molar ratio Et₂Zn/benzaldehyde/chiral ligand of catalyst = 2/1/0.1.

^b Determined by GC (30 m, Chiral Cyclodex-B column, Agilent).

^c Absolute configuration assigned by comparison to the literatures.

(1*S*,2*R*)-(+)-**1** with diethylzinc, the role of the hydroxyl function is of prime importance in good enantiomeric excess. The concentration of efficient (1*S*,2*R*)-(+)-**1** on the surface diluted by ethyl organic moieties leads to lower enantiomeric excess. The hybrid chiral zirconium phosphonate **5a** and **5b** with 62% and 19% molar amounts of (1*S*,2*R*)-(+)-**1**, respectively, conducted the enantiomeric excess to 28% and 22% e.e. (Table 3, entries 3 and 4). Instead of organic ethylphosphonate with inorganic phosphite in hybrid chiral zirconium phosphonates **5**, no enantiomeric excess was obtained (Table 3, entry 5). This maybe due to the exposure of the P–O in phosphite which can catalyze the alkylation of benzaldehyde without enantioselectivity.

3.5.2. The reusability of catalyst

From Table 4, it was found that the catalytic activities and enantioselectivities of chiral zirconium phosphonate (1*S*,2*R*)-(+)-**4a** strongly decrease from 46% to 36% e.e., which may be due to the dilution of zinc oxide formed in the addition of Et₂Zn to benzaldehyde, the loss of the catalyst and the decomposition of zirconium frame. In an effort to understand the true mechanism of loss catalytic activities and enantioselectivities and reconstruction of chiral zirconium phosphonates was under investigation.

4. Conclusion

A new type of self-assembled chiral zirconium phosphonates and hybrid chiral zirconium phosphonates had been prepared by immobilizing (1*S*,2*R*)-(+)-2-amino-1,2-diphenylethanol and (1*R*,2*S*)-(–)-2-amino-1,2-diphenylethanol into the layered zirconium phosphonate framework. Those chiral zirconium phosphonates **4a** and **4b** and hybrid zirconium phosphonates **5a** and **5b** are layered materials with different interlayer spacings attributed to molar ratio of (1*S*,2*R*)-(+)-**1** to ethyl organic moieties. It was shown that the self-assembled zirconium phos-

phonates with chiral 2-aminoalcohol auxiliary led to active heterogeneous catalysis for asymmetric additions of diethylzinc to benzaldehydes with 91% yield and e.e. values of up to 51% which only decreased at 6% enantiomeric excess lower than those in homogeneous asymmetric catalysis.

Acknowledgement

The authors acknowledge the support by the Science Foundation of southwest university.

References

- [1] C. Brown, Chirality in Drug Design and Synthesis, Academic Press, New York, 1990.
- [2] R. Noyori, Asymmetric Catalysis in Organic Synthesis, Wiley, New York, 1994.
- [3] C. Halm, Kurth, M.J. Angew. Chem. Int. Ed. Engl. 37 (1998) 510–512.
- [4] K. Soai, S. Niwa, M.J. Watanabe, Org. Chem. 53 (1988) 927–928.
- [5] W. David, L. Sung, P. Hodge, P.W. Stratford, J. Chem. Soc., Perkin Trans. 1 (1999) 1463–1472.
- [6] M.I. Burguete, E. Garcia-Verdugo, M.J. Vicent, S.V. Luis, H. Pennemann, N.G. Keyserling, J. Martens, Org. Lett. 22 (2002) 3947–3950.
- [7] K. Soai, M. Watanabe, A. Yamamoto, J. Org. Chem. 55 (1990) 4832–4835.
- [8] N. Bellocq, S. Abramson, M. Laspéras, D. Brunei, P. Moreau, Tetrahedron-Asymmetry 10 (1999) 3229–3241.
- [9] S. Abramson, M. Laspéras, A. Galarneau, D. Desplandier-Giscard, D. Brunei, Chem. Commun. (2000) 1773–1774.
- [10] S. Abramson, M. Laspéras, B. Chiche, J. Mol. Catal. A. 165 (2001) 231–242.
- [11] R.I. Kureshy, I. Ahmad, N.H. Khan, S.H.R. Abdi, K. Pathak, R.V. Jasra, J. Catal. 238 (2006) 134–141.
- [12] A. Clearfield, R.H. Blessing, J.A. Stynes, J. Inorg. Nucl. Chem. 30 (1968) 2249–2258.
- [13] J.M. Troup, A. Clearfield, Inorg. Chem. 16 (1977) 3311–3314.
- [14] D.M. Poojary, B.G. Shepizer, A. Clearfield, J. Chem. Soc. Dalton Trans. 1 (1995) 111–113.
- [15] M.B. Dines, P.M. Digiacomio, Inorg. Chem. 20 (1981) 92–97.
- [16] K. Segawa, Y. Ban, Hyomen Kagaku 16 (1995) 80; K. Segawa, Y. Ban, Chem. Abst. 124 (1996) 218390.
- [17] I.O. Benftez, B. Bujoli, L.J. Camus, C.M. Lee, F. Odobel, D.R. Talham, J. Am. Chem. Soc. 124 (2002) 4363–4370.
- [18] I.C. Marcu, I. Sandulescu, J.M.M. Millet, Appl. Catal. 227 (2002) 309–320.
- [19] M. Curini, F. Montanari, O. Rosati, E. Lioy, R. Margarita, Tetrahedron Lett. 44 (2003) 3923–3925.
- [20] Y. Sui, X.K. Fu, J.R. Chen, X.B. Ma, R.Q. Zeng, Mater. Lett. 59 (2005) 2115–2119.
- [21] R.Q. Zeng, X.K. Fu, C.B. Gong, Y. Sui, X.B. Ma, X.B. Yang, J. Mol. Catal. A 229 (2005) 1–5.
- [22] M. Karlsson, C. Andersson, J. Hjortkjaer, J. Mol. Catal. A 166 (2001) 337–343.
- [23] X.B. Ma, X.K. Fu, J. Mol. Catal. A 208 (2004) 129–133.
- [24] C. Massimo, M. Trancesca, R. Ornelio, L. Eduardo, M. Roberto, Tetrahedron Lett. 44 (2003) 3923–3925.
- [25] H.L. Ngo, H. Aiguo, W.B. Lin, J. Mol. Catal. A 215 (2004) 177–186.
- [26] A.K. Bhattacharya, G. Thyagarajan, Chem. Rev. 81 (1981) 415–430.
- [27] D.J. MacLalchlan, K.R. Morgan, J. Phys. Chem. 96 (1992) 3458–3464.
- [28] A. Clearfield, J.D. Wang, Y. Tian, E. Stein, C. Bhardwaj, J. Solid State Chem. 117 (1995) 275–289.
- [29] M. Kitaura, S. Suga, R. Kawai, R. Noyori, J. Am. Chem. Soc. 108 (1986) 6071–6072.